CHAPTER VI

POLYDIPHENYLAMINE/ZEOLITE Y COMPOSITE AS A SENSOR ARRAY FOR THE SELECTION OF DIFFERENT CHEMICAL VAPORS

6.1 Abstract

A composite of nanoscale polydiphenylamine (nPDPA) and dealuminated zeolite Y (DYH[80]) was fabricated to be used as a sensor array for discriminating various kinds of chemical solvent vapors: non polar solvents, low polar solvents, and high polar solvents. Discriminant analysis was used to confirm that the composite could distinguish different chemical solvents. The effects of surfactant type and concentration, and DYH[80] content on the electrical conductivity responses, sensitivity, and selectivity of the composite were investigated. The induction and recovery time, and cyclic response of the composite were also investigated. The composite with sodium dodecyl sulfate as a surfactant with 15 %v/v DYH[80] showed relatively high sensitivity toward dichloromethane (DCM) vapor. Discriminant analysis confirmed that the response patterns of the composite toward each chemical solvent could be distinguished among non polar and low polar solvents, but not high polar solvents. Moreover, the interaction of the composite and DCM vapor was reversible as confirmed by cyclic response, Fourier transform infrared spectroscopy spectra, and electrostatic force microscopy images. When compared with conventional microscale polydiphenylamine (cPDPA) composites, the nanoscale polydiphenylamine composite with dealuminated zeolite Y (nPDPA/DYH[80]) is a promising material for use as a sensor array for detecting non polar and low polar solvents.

Keywords: Polydiphenylamine; Zeolite Y; Sensor array; Chemical vapor; Discriminant analysis

6.2 Introduction

Chemical vapor intrusion is of concern because chemical vapors may cause many health problems (e.g., eye and respiratory irritation, headaches, nausea, cancer or chronic disease) (EPA, 2012). Health risks are dependent on the type and amount of chemical vapor exposure (NAOAA, 2012). Generally, chemical vapors can originate from common household products (e.g., paint, paint stripper and thinner, new carpeting and furniture, air fresheners, cleaning products, etc.) (EPA, 1991; Sidebottom et al., 2011). Rapid, sensitive, portable, and inexpensive sensor systems are an urgent need to identify a wide range of chemical vapors (Askim et al., 2013; Grate et al., 2001; Janata et al., 2001). Recently, they have been many efforts to develop sensor array systems for many types of materials such as metal oxide semiconductors (Tomchenko et al., 2003), field effect transistors (FET) (Ho, 2011; Potyrailo et al., 2011; James et al., 2005), chemical field-effect transistors (ChemFET) (Janata and Josowicz, 2009; Ronkainen et al., 2010), as well as conductive polymer sensors (Nambiar et al., 2011; Chanthaanont et al., 2012; Konkayan et al., 2013; Kamonsawas et al., 2010; Permpool et al., 2013; Jian et al., 2010; Jun et al., 2009). The sensors based on conductive polymers possess cost effectiveness, better processability, greater sensitivity, and reproducibility than sensors made from inorganic oxides (Partridge et al., 2000). A highly sensitive sensor system improves with the material surface area to mass ratio. Conductive polymers have been developed at nanoscale: nanowires (Huang et al., 2010; Wang et al., 2014; Hangarter et al., 2010), nanotubes (Kwon et al., 2012), nanofibers (Nicholas, 2013; Huang et al., 2002), etc. Another important property of a sensor system is selectivity (Askim et al., 2013). Zeolites are of interest as a selective material because they provide optimal sizes and shapes, which can absorb chemical vapor molecules while sustaining a high surface area to mass ratio due to its porous structure (Zhou et al., 2003). Recently, conductive polymer/zeolite composites have been used as a selective material for many toxic gases: e.g., poly(3,4-ethylenedioxythiophene)-polystyrene sulfonate/zeolite ZSM5 as a carbon monoxide sensor (Chanthaanont et al., 2012); poly(3-thiopheacetic acid)/zeolite Y composite as

an ammonia sensor (Konkayan *et al.*, 2013); polypyrrole/zeolite 3A as a chemical lacquer thinner sensor (Wannatong *et al.*, 2008). etc.

Additionally, a polydiphenylamine/zeolite Y composite with a Si/Al ratio of 80 (D-PDPA/YH[80]) was investigated in terms of electrical conductivity response and sensitivity toward halogenated solvents (Permpool *et al.*, 2013). It was possible to change the selectivity toward polar (e.g. dichloromethane; DCM) and non-polar (e.g. hexane) solvents. However, the sensitivity and selectivity of the composite toward those solvents were low. Thus, a modification of the structure of PDPA and YH[80] was required to enhance the sensitivity toward those vapors. PDPA was synthesized via emulsion polymerization to obtain PDPA at nanoscale (nPDPA). Zeolite Y was modified by a dealumination process (DYH[80]) to increase its hydrophobicity. The objective of the present work, nPDPA and DYH[80] were incorporated together to form a compressed composite to be used as a sensor array to discriminate between different halogenated solvents.

6.3 Experimental

6.3.1 Materials

Diphenylamine, DPA (reagent, Sigma Aldrich), ammonium persulfate, $(NH_4)_2S_2O_8$, (AR grade, Riedel-deHaën), and 36.5–38.0 %w/w hydrochloric acid, HCl, (ACS reagent, J.T. Baker) were used for PDPA synthesis. Zeolite Y (Zeolite International) with H^+ as a cation, possessed the Si/Al ratio of 80 (YH80) in powder form. Sodium dodecyl sulfates, SDS, (Lobachemie), Cetyltrimethylammonium bromide, CTAB, (Sigma Aldrich), Polyoxyethylene (20) sorbitan monooleate, TW80, (ICI Americas, Inc.) were used as surfactants and dopants. The solvents for the sensitivity tests were hexane, toluene, chloroform, dichloromethane, DCM, tetrahydrofuran, THF, acetone, dimethylformamide, DMF, ethanol, methanol, and propanol. All solvents were of analytical grade and were used as received.

6.3.2 Sample Preparation

Polydiphenylamine nanoparticle (nPDPA) was synthesized via the emulsion polymerization method according to the procedure of Permpool *et al.* (2014). SDS. CTAB. and TW80 were used as soft templates for control size and shape of nPDPA. Zeolite Y was modified through an acid treatment process by varying acid treatment times as previously reported (Permpool *et al.*, 2013). In order to prepare the nPDPA/DYH[80] composites. nPDPA powder was ground with DYH[80] at various concentrations (5. 10. 15. 20. 25. 30. and 50 %v/v). The pellet form of each sample for the conductivity and sensitivity measurement was prepared by pressing with a hydraulic press (GRASEBY SPECAC) under a 4-5 ton load. The diameter of the pellets was ~1.30 cm.

6.3.3 Characterization

The morphology of nPDPA. DYH80 and its blends were investigated by using a scanning electron microscope. SEM (HITACHI. S-4800) with a magnification of 10000x and 30000x. operated at 10 kV.

The charge distribution along the composite backbone before. during. and after exposure to DCM. THF, and acetone was measured by electrostatic force microscopy. EFM (Park System. XE-100) operating in standard EFM mode with an NSC 14=Cr-Au tip. a scan size of 2 mm ⋅ 2 mm, and a scan rate of 0.1 Hz. Voltage was applied to the sample at 5 V. The EFM phase image exhibited brighter regions. which identified positive charges within the composites. while the darker regions identified negative charges within the composite. The degree of charge generated on the surface of the composite was also measured and analyzed.

The chemical interaction between the composites and the vapors was investigated by using Fourier transform infrared spectroscopy. FT-IR (Thermo Nicolet. Nexus 670) in a wave number range of 4000–600 cm^{-1}. a resolution of 4 cm^{-1}. and a scan number of 64.

6.3.4 Conductivity & Sensitivity Measurement

The conductivity measurement of all PDPA samples was measured by a custom-built two point probe connected with a conductivity meter (KEITHLEY

6517A). Voltage was applied to the sample in the linear Ohmic regime. The resultant current signal was recorded with 6517 Hi-R Test software. Each sample disc was compressed to a diameter of ~1.30 cm and a thickness of ~0.05-0.07 cm as measured with a digital thickness gauge (PEAACOCK. model PDN-20). Electrical conductivity (σ) of the samples was calculated by the following Eq. (6.1);

$$\sigma = \left(\frac{I}{KVt}\right) \tag{6.1}$$

where I is the measured current (A), V is the applied voltage (V). t is the sample thickness (cm). and K is the geometric correction factor which is equal to the ratio w/l, where w and l are the probe width and the length, respectively (1.07×10^{-4}).

Sensitivity of the samples is defined as the change in conductivity of all samples ($\Delta\sigma$) when exposed to the solvents divided by the conductivity value in pure nitrogen. The difference in the specific electrical conductivity (S/cm) was calculated by Eq. (6.2):

$$\Delta\sigma = \sigma_{solvent\ vapor} - \sigma_{N2\ initial} \tag{6.2}$$

where $\sigma_{N2.\ initial}$ is the specific electrical conductivity in N_2 before exposure (S/cm). and $\sigma_{solvent\ vapor}$ is the specific electrical conductivity (S/cm) under solvent exposure at various concentrations. All measurements were taken at 27 ± 1 °C. at atmospheric pressure (atm) using a 5 L/min air and N_2 flow rate.

6.4 Results and Discussions

6.4.1 Sensitivity of nPDPA toward DCM Vapor: Effect of Surfactant Type and Content

Sensitivity values of nPDPA toward DCM vapor at various surfactant types and concentrations are shown in Figure 1. The sensitivity values of nPDPA at various surfactants toward DCM vapor increased from $(-6.21 \pm 2.35) \times 10^{-2}$ to $(-9.76 \pm 0.32) \times 10^{-1}$ for nPDPA-SDS. from $(-1.64 \pm 0.04) \times 10^{-2}$ to $(-3.19 \pm 0.82) \times 10^{-1}$ for

nPDPA-CTAB. and from $(-1.21 \pm 0.01) \times 10^{-2}$ to $(-2.19 \pm 0.36) \times 10^{-1}$ for nPDPA-TW80 with increasing monomer to surfactant mole ratio from 1:0.001 to 1:0.5 (CMC point). But values decreased to $(-3.71 \pm 1.15) \times 10^{-1}$ for nPDPA-SDS. (-7.17 ± 0.40) $\cdot \ 10^{-2}$ for nPDPA-CTAB. and $(-6.01 \pm 1.05) \cdot 10^{-2}$ for nPDPA-TW80 when the monomer to surfactant mole ratio was equal to 1:1. This is because the particle size of nPDPA decreases with increasing surfactant concentration until reaching the CMC point of each surfactant (Permpool *et al.*. 2014). The CMC points are 3.5×10^{-5} mol/l. 4.12×10^{-4} mol/l. and 8.092×10^{-3} mol/l for SDS. CTAB. and TW80. respectively. The smaller particle size of nPDPA provided larger surface area for electron transfer, hence sensitivity increased (Wannatong *et al.*. 2008). Moreover, electrical conductivity sensitivity of nPDPA-SDS toward DCM vapor was higher than that of nPDPA-CTAB. and nPDPA-TW80, respectively, as shown in Figure 1. This is due to a difference in: (i) the strength of the intermolecular interaction between the polymers and the vapors: (ii) steric effect of surfactant molecules. Stronger interactions between the polymers and vapors induced greater sensitivity (Askim *et al.*. 2013). For nPDPA-SDS and nPDPA-CTAB. the interaction between the polymers and the vapors was a ion-dipole interaction (~40-600 kJ/mole per interaction) (Silberberg. 2006). But the interaction between nPDPA-TW80 and the DCM vapor was the dipole-dipole interaction (~5-25 kJ/mole per interaction) (Silberberg. 2006). So. nPDPA-SDS. and nPDPA-CTAB were expected to have a sensitivity value toward DCM vapor higher than that of nPDPA-TW80. In addition. electron mobility along the polymer chain was obstructed due to the steric effect of each surfactant molecule. The molecular size of TW80 was larger and thus it had a greater steric effect than those of CTAB. and SDS. respectively. Consequently. the electron mobility along the nPDPA-TW80 backbone was more obstructen than nPDPA-CTAB and nPDPA-SDS. In comparison to the conventional micro scale of PDPA (cPDPA). sensitivity of nPDPA-SDS toward DCM $[(- 9.76 \pm 0.32) \times 10^{-1}]$ is higher than that of cPDPA $[(-3.83 \pm 0.15) \times 10^{-2}]$ at 39.24%.

6.4.2 Sensitivity of nPDPA/DYH[80] Composite toward DCM Vapor: Effect of DYH[80] Content

In order to improve selectivity of the nPDPA. zeolite Y was employed and investigated further. Sensitivity values of nPDPA/DYH[80] composite toward DCM vapor at various DYH[80] zeolite concentrations are shown in Figure 2. Sensitivity values of the composites increase from $(-1.19 \pm 0.57) \times 10^{-1}$ to $(-9.764 \pm 0.32) \times 10^{-1}$ for the nPDPA-SDS/DYH[80] composite. from $(-3.22 \pm 3.03) \times 10^{-1}$ to $(-6.74 \pm 1.40) \times 10^{-1}$ for the nPDPA-CTAB/DYH[80] composite. and from $(-4.57 \pm 5.40) \times 10^{-3}$ to $(-2.10 \pm 2.56) \times 10^{-2}$ for the nPDPA-TW80/DYH[80] composite with increasing DYH[80] concentration from 5 %v/v to 15 %v/v. As DYH80 concentration increases to 30 %v/v, sensitivity decreases to $(-1.64 \pm 0.73) \times 10^{-1}$ for the nPDPA-SDS/DYH[80] composite. $(-4.46 \pm 1.07) \times 10^{-1}$ for the nPDPA-CTAB/DYH[80] composite, and $(-1.65 \pm 1.04) \times 10^{-2}$ for the nPDPA-TW80/DYH[80] composite. Sensitivity of the nPDPA-SDS/DYH[80] composite toward the DCM vapor is also higher due to the difference in the strength of the intermolecular interaction between the polymers and vapors. as well as the steric effect of surfactant molecules. The initial increases in sensitivity of the composite. as DYH[80] concentration increased from 5 %v/v to 15 %v/v, are due to the DCM molecules being trapped in the micro porous structure of DYH[80]. With a higher DYH[80] concentration. more DCM molecules could be trapped in the DYH[80] zeolite (Zheng et al.. 2013). Nevertheless, when the DYH[80] concentration increased to 30 %v/v, sensitivity of the composite decreased because the active sites of the polymer were reduced (Phumman et al.. 2009). As compared to our previous work, the nPDPA-SDS composite with 15 %v/v DYH[80] promoted the highest sensitivity toward DCM vapor while the highest sensitivity toward DCM vapor of the cPDPA/DYH[80] composite came from 30 %v/v DYH[80]. The nPDPA-SDS/DYH[80] composite showed higher sensitivity toward DCM vapor than the cPDPA/DYH[80] composite by ~45% due to the synergistic effects between the nanoparticles of nPDPA-SDS and greater hydrophobicity of DYH[80] (Saidina and Anggoro. 2002: Holmberg et al.. 2004: Kumar et al.. 2000: Triantafillidis et al., 2000). In summary. the nPDPA-SDS/DYH[80] composite was more effective and could be used more efficiently as a sensing material for DCM vapor than

cPDPA/DYH[80] composite. The nPDPA with the monomer to SDS ratio of 1:0.5 and 15 %v/v DYH[80] (nPDPA-SDS_1-0.5/15%DYH[80]) was employed for further investigation.

6.4.3 Sensitivity of nPDPA-SDS_1-0.5-15%DYH80 Composite toward Various Solvent Vapors

Sensitivity of the nPDPA-SDS_1-0.5/15%DYH[80] composite toward different kinds of chemical vapors was measured to test its ability to discriminate different analytes. Figure 3 shows sensitivity values of the composite toward three different groups of chemical vapors: (i) high polar solvents—methanol, ethanol, and propanol; (ii) low polar solvents—dichloromethane, DCM, tetrahydrofuran, THF, acetone, and dimethylformamide, DMF, and; (iii) non polar solvents—hexane, toluene, and chloroform. The composites show negative responses toward all chemical vapors. The largest responses are toward the low polar solvents (DCM>THF>acetone>DMF), followed by non polar solvents (toluene≈chloroform>hexane). The composite possessed low sensitivity toward the high polar solvents. The sensitivity values of the composite toward all chemical vapors are tabulated in Table 1. Typically, a chemical polymeric sensor is molecular recognition device that responds to a specific interaction between the polymer and target vapor (Hunter, 2004; Rigby, 1986; Müller and Hobza, 1999). The low polar solvents, the interaction between the composite and the vapors is quite strong via the ion-dipole interaction. The non polar solvents have a low dielectric constant and dipole moment. The interaction between the composite and the vapors occurs through the physical adsorption on the surface of the composite. For the high polar solvent, the interaction between the composite and the vapors resulted in the hydrogen bonding because the vapors had a high dielectric constant and high dipole moment. From this conjecture, the sensitivity of the composite toward different chemical vapors should be in the order of: high polar solvent>low polar solvent>non polar solvent. However, the results showed that the composite has rather low sensitivity toward high polar solvents relative to that of the low polar solvents, and the non polar solvents. Not only the specific interaction between the composite and the target vapor can affect its sensitivity, but the solute-solvent interaction is also

dominant (Rigby. 1986; Harada *et al.*, 2011; Guan *et al.*, 2008). The Hansen solubility parameter, δ, is used to indicate solvency behavior of a specific solvent (Bruke, 1984). Materials are miscible when δ is similar (Hansen. 1967, 2012). The solubility parameter of nPDPA is 20.8 $MPa^{1/2}$ (Permpool *et al.*, 2013). As shown in Table 2, the solubility parameter of high polar solvents is quite different from that of nPDPA. But solubility parameters of the low polar and non polar solvents are not much different from that of nPDPA. Consequently, the composite could not dissolve in a high polar solvent as sensitivity values of the composite toward these solvents are very low. This caused the order of sensitivity to be: low polar solvent>non polar solvent>high polar solvent.

6.4.4 The Temporal Response of the nPDPA-SDS_1-0.5/15%DYH[80] Composite toward Various Solvent Vapors

Table 1 shows the induction and recovery times of the composite when exposed to 10 chemical vapors. For the non polar solvents, the induction time of the composite is 12.94 ± 0.72 min for hexane, 7.79 ± 0.32 min for toluene, and 7.54 ± 0.16 min for chloroform. For the low polar solvents, the induction time of the composite is 5.31 ± 0.07 min for DCM, 6.78 ± 0.48 min for THF, 7.88 ± 0.49 min for acetone, and 6.95 ± 0.57 min for DMF. For the high polar solvents, the induction time of the composite is 10.84 ± 0.55 min for methanol, 10.94 ± 0.69 min for ethanol, and 11.34 ± 0.86 min for propanol. Thus, the composite shows the lowest induction times toward the low polar solvents, followed by the non polar solvents, and the high polar solvents, respectively. The recovery time of the composite follows the same behavior as the induction time: the low polar solvents have the lowest recovery times, followed by the non polar solvents, and the high polar solvents, respectively. Since the interaction between the composite and the low polar and non polar solvents causes a dipole-dipole interaction, this lowers the induction and recovery times (Askim *et al.*, 2013). On the other hand, for the high polar solvents, the interaction of the composite and the vapors is through the hydrogen bonding which consumes high energy per mole of interaction but it cannot dissolve in the composite due to the solvency behavior. So, the induction and recover times of the composite toward the high polar solvents are relatively higher than those of the other

two types of solvents. In comparison with our previous work, the induction and recovery times toward the DCM vapor of cPDPA composite with DYH[80] was 15.61 ± 0.07 min, and 12.81 ± 0.08 min, respectively. The cPDPA/DYH[80] composite showed lower induction and recovery times toward DCM vapor than nPDPA-SDS_1-0.5/15%DYH[80] composite used in this work due to lower surface area in comparison to the nanoscale PDPA composite.

6.4.5 Discriminant Analysis of nPDPA-SDS_1-0.5/15%DYH[80] Composite toward DCM, THF, and Acetone

Since the composite has different sensitivity responses toward various kinds of solvent vapors, the statistical technique was used to estimate the sensitivity responses generated by the composite, which can be used to discriminate different solvents. The data were transformed to a canonical score by linear discriminant analysis (LDA) (Askim et al., 2013; Cooper et al., 2010) as shown in Figure 4. Figure 4a shows the discriminant analysis of the sensitivity response of the nPDPA-SDS_1-0.5/15%DYH[80] composite toward 10 different chemical vapors at a concentration of 50 %v/v. The high polar and non polar solvents are not clearly discriminated and show overlapping between the groups. But the low polar solvents are clearly discriminated from each other as shown in Figure 4b. Therefore, the effect of vapor concentration of the low polar solvent on sensitivity of the composite was investigated next. Figure 5 shows sensitivity of the nPDPA-SDS_1-0.5/15%DYH[80] composite toward DCM, THF, and acetone vapor at different concentrations at 27 ± 1 °C and 1 atm. Sensitivity of the composite exposed to DCM increases from -0.082 ± 0.066 to -0.976 ± 0.738 as the vapor concentration increases from 5 %v/v (7.696 ppm) to 100 %v/v (153.914 ppm) (Figure 5). For THF exposure, sensitivity increases from -0.053 ± 0.053 to -0.476 ± 0.491 as the vapor concentration increases from 5 %v/v (1.583 ppm) to 100 %v/v (31.668 ppm). For acetone exposure, sensitivity increases from -0.009 ± 0.0300 to -0.117 ± 0.321 as the vapor concentration increases from 5 %v/v (2.428 ppm) to 100 %v/v (38.577 ppm). Thus the composite shows linear responses in relation to vapor concentrations. The slope of each graph indicates selectivity of the composite toward the vapors (Ma et al., 2011). The slope of DCM (-3×10^{-5}) is greater than that of THF (-2×10^{-5}), and

acetone (-5×10^{-6}), respectively. This suggests that the selectivity of the composite toward DCM is higher than that of THF and acetone. Moreover, the limit of detection (LOD) of the composite was also investigated. LOD is the estimate from the mean of the nitrogen gas (blank), and the standard deviation of nitrogen gas and target vapors (Loock et al., 2012). The average LOD of the composite was 225 ppm for DCM, 150 ppm for THF, and 1070 ppm for acetone.

6.4.6 Cyclic Response and Chemical Reaction between nPDPA-SDS_1-0.5/ 15%DYH[80] Composite and Vapor

Figure 6 shows the electrical conductivity of the composite toward DCM. The measurement was repeated for 5 cycles. The composite shows a negative cyclic response when exposed to DCM. The conductivity values of the composite of the 1st, 2nd, 3rd, 4th, and 5th cycle are $8.74 \pm 0.69 \times 10^{-5}$ S/cm, $8.79 \pm 0.05 \times 10^{-5}$ S/cm, $9.49 \pm 1.27 \times 10^{-5}$ S/cm, $9.02 \pm 0.74 \times 10^{-5}$ S/cm, and $8.96 \pm 0.87 \times 10^{-5}$ S/cm, respectively. This suggests that the interaction between the composites and the vapors is quite reversible. Moreover, the FT-IR spectra of the composite before, during, and after exposure to DCM vapor confirm the interaction between the composite and the vapor, as shown in Figure 7. Before DCM exposure, the spectrum shows characteristic peaks of D-PDPA and DYH[80] (Santana and Dias, 2003; Hua and Ruckenstein, 2003; Sathiyanarayanan et al., 2006). During DCM exposure, new peaks appear at 2974, 2866, 1056, and 1012 cm^{-1}, which can be assigned to the interaction between DCM and D-PDPA, specifically CH_2 in DCM (Lambert et al., 2010). After flushing DCM vapor with N_2, the peaks that correspond to the interaction between the composite and the vapor disappear from the spectrum. This indicates that the interaction between the composite and the vapor is reversible. The charge distribution on the surface of the composite was investigated by the EFM technique with an external electric excitation of 5 volts. Figures 8a-c shows the charge distributions on the surfaces of the composites before, during, and after exposure to DCM. The bright region indicates positive charges on the surface while the dark region indicates negative charges on the surface. Before exposure to DCM (Figure 8a), both bright and dark regions are observed on the surface of the composite. This indicates that the composite backbone has both positive and negative

charges present. During exposure to DCM (Figure 8b). there are more dark regions. This indicates that the composite accommodates electrons from the DCM vapor. After exposure to DCM (Figure 8c). the image shows both bright and dark regions equally, which implies that the composite has no additional electrons left on its surface. This further proves that the interaction between the polymer and the vapor is reversible. Figure 9 shows the proposed mechanism of the composite and DCM vapor. The chlorine atom of DCM is an electron donating group. It will stabilize the cations of the imine nitrogen in the composite. In comparison to our previous work. in which the interaction between the DCM and the cPDPA/DYH[80] composite is irreversible, the interaction in this work is reversible due to the weak interaction between the composite and the vapor as described above. The weak interaction of the composite and the vapor occurs due to the steric effect of the SDS molecules causing only physical adsorption on the composite.

6.5 Conclusions

By means of nanoscale PDPA particles in the nPDPA-SDS_1-0.5/15%DYH[80] composite. sensitivity and selectivity of the composite toward various kinds of chemical vapors were drastically improved. Sensitivity toward DCM of the nPDPA-SDS_1-0.5/15%DYH[80] composite was as high as 39.24% compared with that of the cPDPA. With increasing zeolite concentration. sensitivity of the composite increased because more vapor molecules were trapped in DYH80. The DYH80 zeolite concentration which showed the highest sensitivity toward DCM in nPDPA-SDS_1-0.5/15%DYH[80] was lower than that of cPDPA/30%DYH[80] with a higher sensitivity toward DCM vapor of 45.49%. due to the synergistic effect between nPDPA-SDS and DYH[80]. Moreover. the nanoscale composite showed lower induction and recovery times toward the chemical vapors relative to those of the cPDPA/DYH[80] composite due to the weaker interaction between the composite and the vapors. The composite showed different electrical conductivity responses toward various kinds of chemical solvents: high polar solvents: low polar solvents: and non polar solvents. With the use of linear discriminant analysis. it was determined that the composite was able to successfully discriminate low polar

solvents from the non polar solvents group. but the case of high polar solvents was not successful. The interaction between the composite and DCM vapors was reversible as confirmed by cyclic response. FT-IR spectra. and EFM images. Based on the results. the composite of nPDPA-SDS_1-0.5/15%DYH[80] is a promising sensing material that can discriminate different kinds of chemical solvents.

6.6 Acknowledgements

6.7 References

Askim. J.R.. Mahmoudi. M.. and Suslick. K.S. (2013) Optical sensor arrays for chemical sensing: the optoelectronic nose. Chemical Society Reviews. 42(22). 8649-8682.

Chanthaanont. P. and Sirivat. A. (2012) Interaction of carbon monoxide with PEDOT-PSS/zeolite composite: effect of Si/Al ratio of ZSM-5 zeolite. e-Polymer. 12(1). 106-116.

Cooper. J.S.. Raguse. B.. Chow. E.. Hubble. L.. Müller. K.H.. and Wieczorek. L. (2010) Gold nanoparticle chemiresistor sensor array that differentiates between hydrocarbon fuels dissolved in artificial seawater. Analytical Chemistry. 82(9). 3788-3795.

de Santana. H. and Dias. F.C. (2003) Characterization and properties of polydiphenylamine electrochemically modified by iodide species. Materials Chemistry and Physics. 82(3). 882-886.

EPA. U. (1991) Needs for eleven TRI organic chemical groups. environmental protection agency. Paper presented at Pollution Prevention Research. Washington. DC. USA.

EPA. U. (2012) What you should know about the problem of vapor intrusion. Paper presented at Pollution Prevention Research. Washington, DC. USA.

Gopel, W. (1995) Nanostructured sensors for molecular recognition. Philosophical Transactions: Physical Sciences and Engineering. 353(1703), 333-354.

Grate, J.W., Kaganove, S.N., and Nelson, D.A. (2001) Polymers for chemical sensors using hydrosilylation chemistry. Report. Pacific Northwest National Laboratory. The U.S. Department of Energy. Washington, USA.

Guan, G., Liu, B., Wang, Z., and Zhang, Z. (2008) Imprinting of molecular recognition sites on nanostructures and its applications in chemosensors. Sensors. 8(12), 8291-8320.

Hangarter, C.M., Bangar, M., Mulchandani, A., and Myung, N.V. (2010) Conducting polymer nanowires for chemiresistive and FET-based bio/chemical sensors. Journal of Materials Chemistry. 20(16), 3131-3140.

Hansen, C.M. (1967) The Three Dimensional Solubility Parameter and Solvent Diffusion Coefficient: their Importance in Surface Coating Formation. Copenhagen: Danish Technical Press.

Hansen, C.M. (2012) Hansen Solubility Parameters: A User's Handbook. Second Edition. New York: Taylor & Francis.

Harada, A., Kobayashi, R., Takashima, Y., Hashidzume, A., and Yamaguchi, H. (2011) Macroscopic self-assembly through molecular recognition. Nature Chemistry. 3(1), 34-37.

Ho, G.W. (2011) Gas sensor with nanostructured oxide semiconductor materials. Science of Advanced Materials. 3(2), 150-168.

Holmberg, B.A., Wang, H., and Yan, Y. (2004) High silica zeolite Y nanocrystals by dealumination and direct synthesis. Microporous and Mesoporous Materials. 74(1–3), 189-198.

Hua, F. and Ruckenstein, E. (2003) Water-soluble conducting poly(ethylene oxide)-grafted polydiphenylamine synthesis through a "Graft Onto" process. Macromolecules. 36(26), 9971-9978.

Huang, J., Virji, S., Weiller, B.H., and Kaner, R.B. (2002) Polyaniline nanofibers: facile synthesis and chemical sensors. Journal of the American Chemical Society. 125(2), 314-315.

Huang, J., Wang, K., and Wei, Z. (2010) Conducting polymer nanowire arrays with enhanced electrochemical performance. Journal of Materials Chemistry. 20(6), 1117-1121.

Hunter, C.A. (2004) Quantifying intermolecular interactions: guidelines for the molecular recognition toolbox. Angewandte Chemie International Edition. 43(40), 5310-5324.

James, D., Scott, S.M., Ali, Z., and O'Hare, W.T. (2005) Chemical sensors for electronic nose systems. Microchimica Acta. 149(1), 1-17.

Janata, J. (2001) Centennial retrospective on chemical sensors. Analytical Chemistry. 73(5), 150 A-153 A.

Janata, J. and Josowicz, M. (2009) Organic semiconductors in potentiometric gas sensors. Journal of Solid State Electrochemistry. 13(1), 41-49.

Kamonsawas, J., Sirivat, A., Niamlang, S., Hormnirun, P., and Prissanaroon-Ouajai, W. (2010) Electrical conductivity response of poly(phenylene-vinylene)/ zeolite composites exposed to ammonium nitrate. Sensors. 10(6), 5590-5603.

Konkayan, S., Chanthaanont, P., Prissanaroon, W., Hormnirun, P., and Sirivat, A. (2013) Ammonia sensing and electrical properties based on composite of poly(3-thiopheneacetic acid) and zeolite Y. Materials Technology. 28(6), 332-338.

Kumar, S., Sinha, A.K., Hegde, S.G., and Sivasanker, S. (2000) Influence of mild dealumination on physicochemical, acidic and catalytic properties of H-ZSM-5. Journal of Molecular Catalysis A: Chemical. 154(1-2), 115-120.

Kwon, O.S., Park, S.J., Lee, J.S., Park, E., Kim, T., Park, H.W., You, S.A., Yoon, H., and Jang, J. (2012) Multidimensional conducting polymer nanotubes for ultrasensitive chemical nerve agent sensing. Nano Letters. 12(6), 2797-2802.

Lambert, J.B., Gronert, S., Shurvell, H.F., and Lightner, D. (2010) Organic Structural Spectroscopy. New Jersey: Prentice Hall PTR.

Loock, H.P. and Wentzell, P.D. (2012) Detection limits of chemical sensors: Applications and misapplications. Sensors and Actuators B: Chemical. 173(0), 157-163.

Ma, W., Yang, H., Wang, W., Gao, P., and Yao, J. (2011) Ethanol vapor sensing properties of triangular silver nanostructures based on localized surface plasmon resonance. Sensors, 11(9), 8643-8653.

Müller-Dethlefs, K. and Hobza, P. (1999) Noncovalent interactions: A challenge for experiment and theory. Chemical Reviews, 100(1), 143-168.

Nambiar, S. and Yeow, J.T.W. (2011) Conductive polymer-based sensors for biomedical applications. Biosensors and Bioelectronics, 26(5), 1825-1832.

National Oceanic and Atmospheric Administration, U.D.o.C., US Goverment. "Immediately Dangerous to Life and Health Limits (IDLHs)." 6 Nov 2012. 7 Nov 2012 <http://response.restoration.noaa.gov/idlhs>

Nicholas, J.P. (2013) Electrospun conducting polymer nanofibers as the active material in sensors and diodes. Journal of Physics: Conference Series, 421(1), 012004.

Paradee, N. and Sirivat, A. (2013) Synthesis of poly(3,4-ethylenedioxythiophene) nanoparticles via chemical oxidation polymerization. Polymer International, 63(1), 106-113.

Partridge, A.C., Jansen, M.L., and Arnold, W.M. (2000) Conducting polymer-based sensors. Materials Science and Engineering: C, 12(1–2), 37-42.

Permpool, T., Sirivat, A., and Aussawasathien, D. (2014) Synthesis of polydiphenylamine with tunable size and shape via emulsion polymerization. Polymer International, (accepted).

Permpool, T., Sirivat, A., Aussawasathien, D., and Wannatong, L. (2013) Development of polydiphenylamine/zeolite Y composite by dealumination process as a sensing material for halogenated solvents. Polymer-Plastics Technology and Engineering, 52, 907-920.

Permpool, T., Supaphol, P., Sirivat, A., and Wannatong, L. (2012) Polydiphenylamine–polyethylene oxide blends as methanol sensing materials. Advances in Polymer Technology, 31(4), 401-413.

Phumman, P., Niamlang, S., and Sirivat, A. (2009) Fabrication of poly(p-phenylene)/zeolite composites and their responses towards ammonia. Sensors, 9(10), 8031-8046.

Potyrailo, R.A., Surman, C., Nagraj, N., and Burns, A. (2011) Materials and transducers toward selective wireless gas sensing. Chemical Reviews. 111(11), 7315-7354.

Rigby, M. (1986) The Forces between Molecules. Oxford: Clarendon Press.

Ronkainen, N.J., Halsall, H.B., and Heineman, W.R. (2010) Electrochemical biosensors. Chemical Society Reviews. 39(5), 1747-1763.

Saidina, A.N.A. and Anggoro, D.D. (2002) Dealuminated ZSM-5 zeolite catalyst for ethylene oligomerization to liquid fuels. Journal of Natural Gas Chemistry. 11(1), 79-86.

Santana, H. and Temperini, M. (1996) The spectroscopic characterization of polydiphenylamine and one of its oligomeric fractions. Journal of the Brazilian Chemical Societies 7(6), 485-490.

Sathiyanarayanan, S., Muthukrishnan, S., and Venkatachari, G. (2006) Synthesis and anticorrosion properties of polydiphenylamine blended vinyl coatings. Synthetic Metals. 156(18–20), 1208-1212.

Sidebottom, H. and Franklin, J. (1996) The atmospheric fate and impact of hydrochlorofluorocarbons and chlorinated solvents. Pure and Applied Chemistry. 68(9), 1757-1769.

Silberberg, M.S. (2006) Principles of General Chemistry. Ohio: McGraw-Hill Higher Education.

Tomchenko, A.A., Harmer, G.P., Marquis, B.T., and Allen, J.W. (2003) Semiconducting metal oxide sensor array for the selective detection of combustion gases. Sensors and Actuators B: Chemical. 93(1–3), 126-134.

Triantafillidis C. S., Vlessidis A. G., and Evmiridis N. P. (2000) Dealuminated H-Y zeolites : Influence of the degree and the type of dealumination method on the structural and acidic characteristics of H-Y zeolites. Industrial & Engineering Chemistry Research. 39(2), 307-319.

Wang, K., Wu, H., Meng, Y., and Wei, Z. (2014) Conducting polymer nanowire arrays for high performance supercapacitors. Small. 10(1), 14-31.

Zheng, Y., Li, X., and Dutta, P.K. (2012) Exploitation of unique properties of zeolites in the development of gas sensors. Sensors. 12(4), 5170-5194.

Zhou, J., Li, P., Zhang, S., Long, Y., Zhou, F., Huang, Y., Yang, P., and Bao, M.
(2003) Zeolite-modified microcantilever gas sensor for indoor air quality
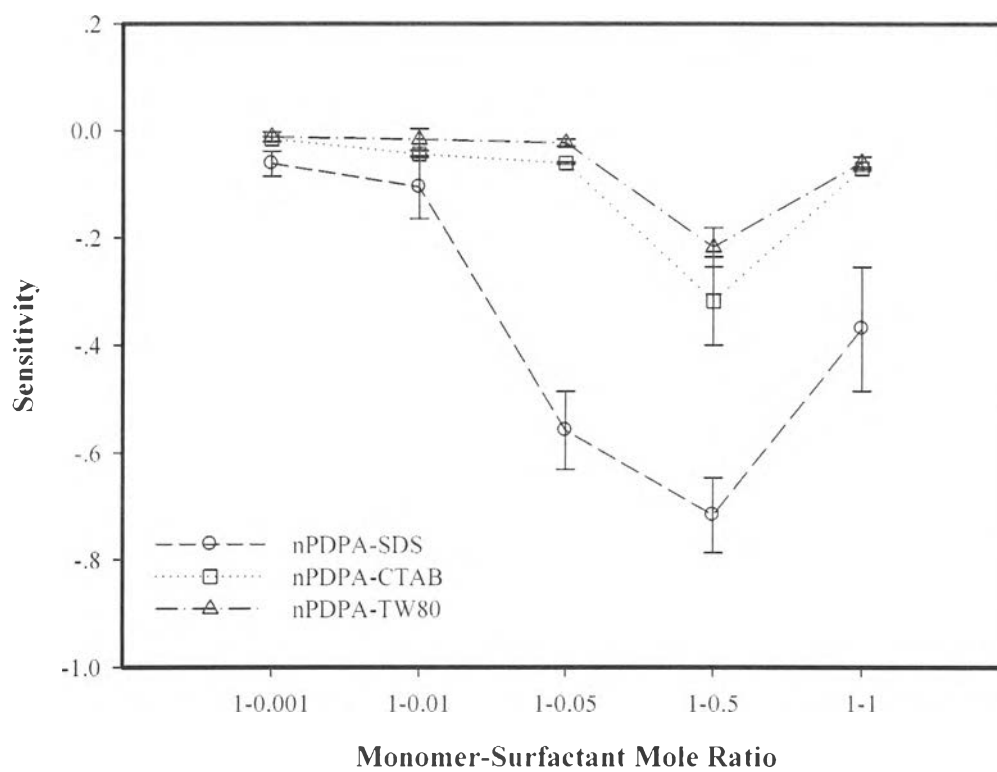control. Sensors and Actuators B: Chemical, 94(3), 337-342.

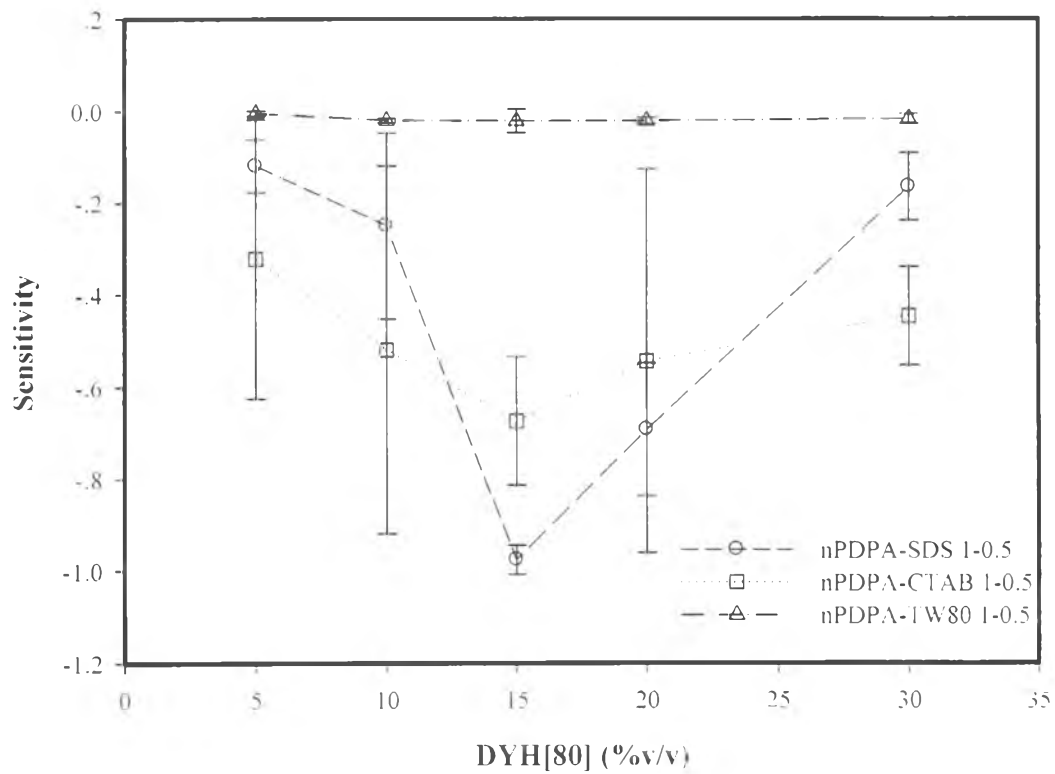**Figure 6.1** Sensitivity of nPDPA toward DCM as a function of surfactant content.

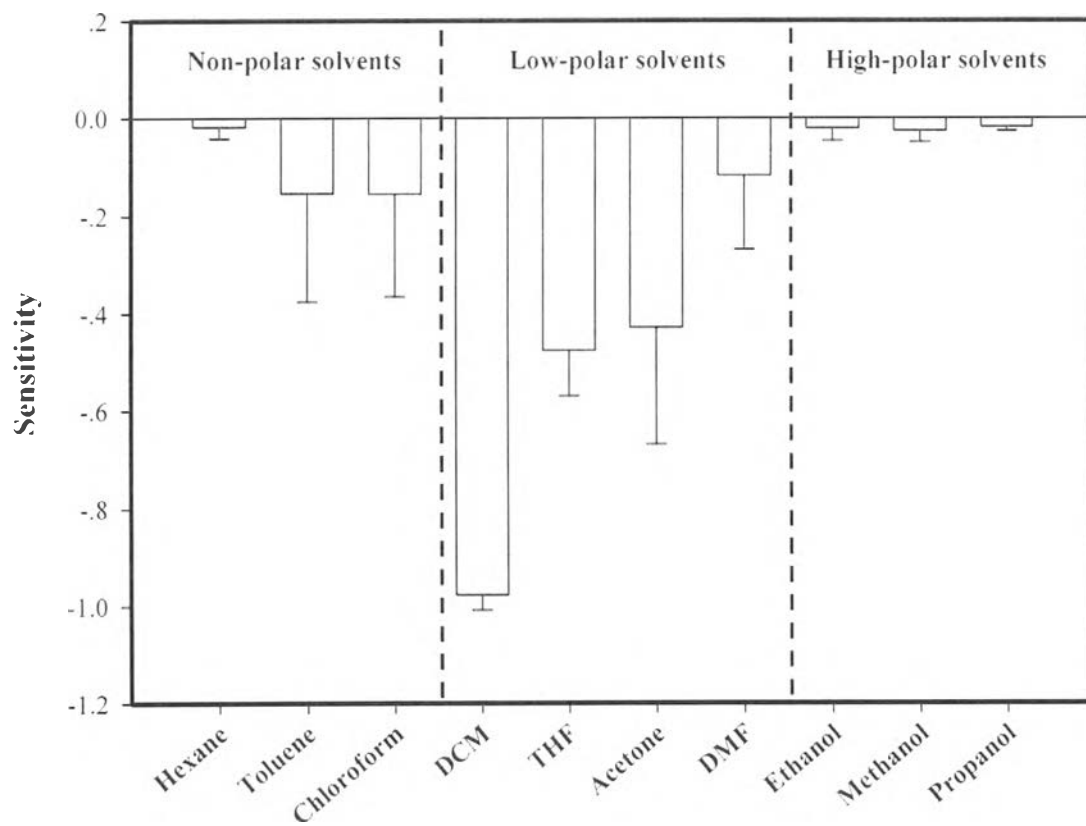**Figure 6.2** Sensitivity of nPDPA/DYH[80] composites toward DCM as a function of DYH[80](12h) content.

Figure 6.3 Sensitivity of nPDPA-SDS_1-0.5/15%DYH[80] composites toward different solvent vapors at 50 %v/v in N_2.
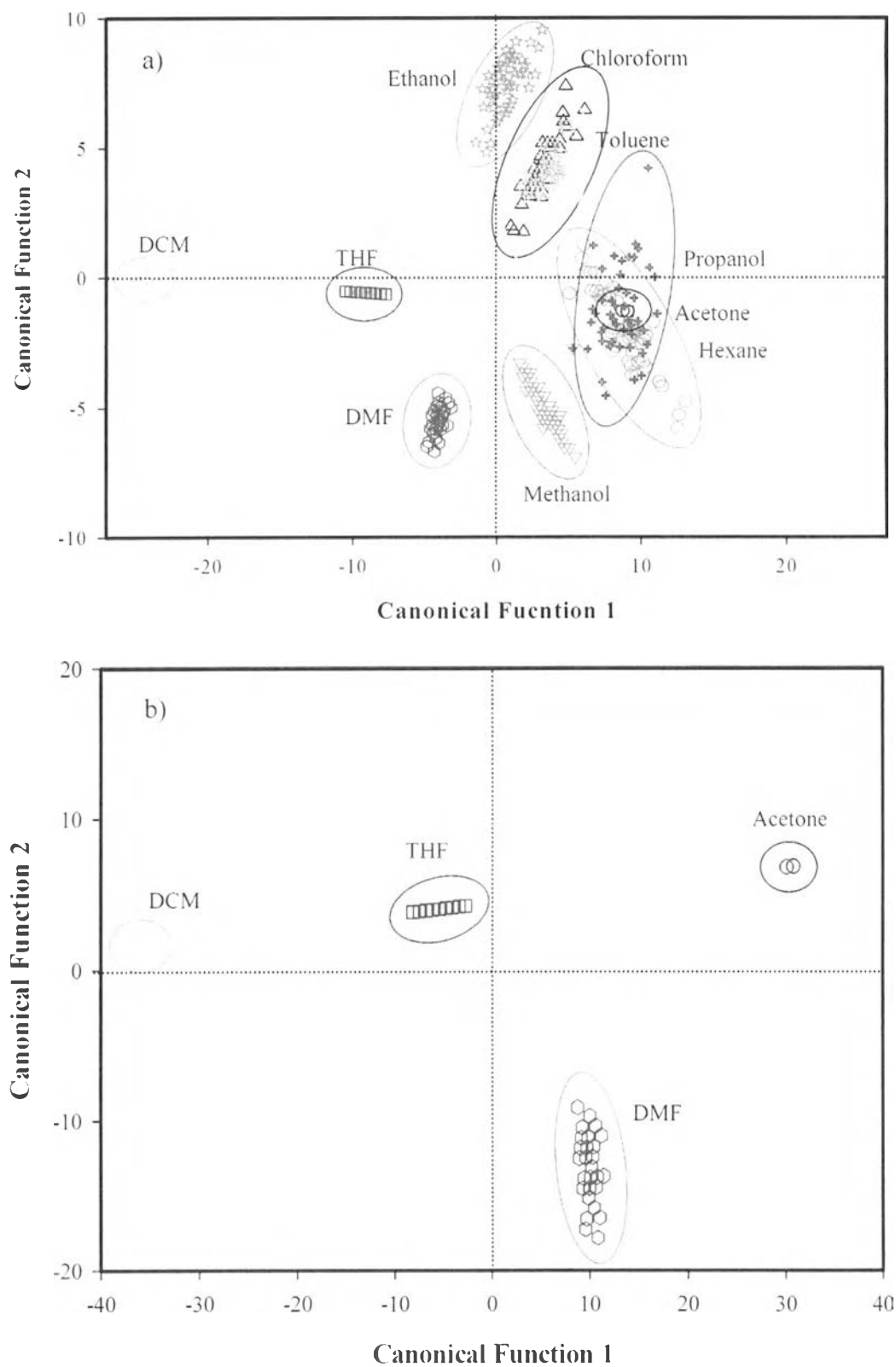
Figure 6.4 Discriminant analysis of sensitivity response of nPDPA-SDS_1-0.5/15% DYH[80] composite toward different 10 vapors; circle indicates the means of the groups.
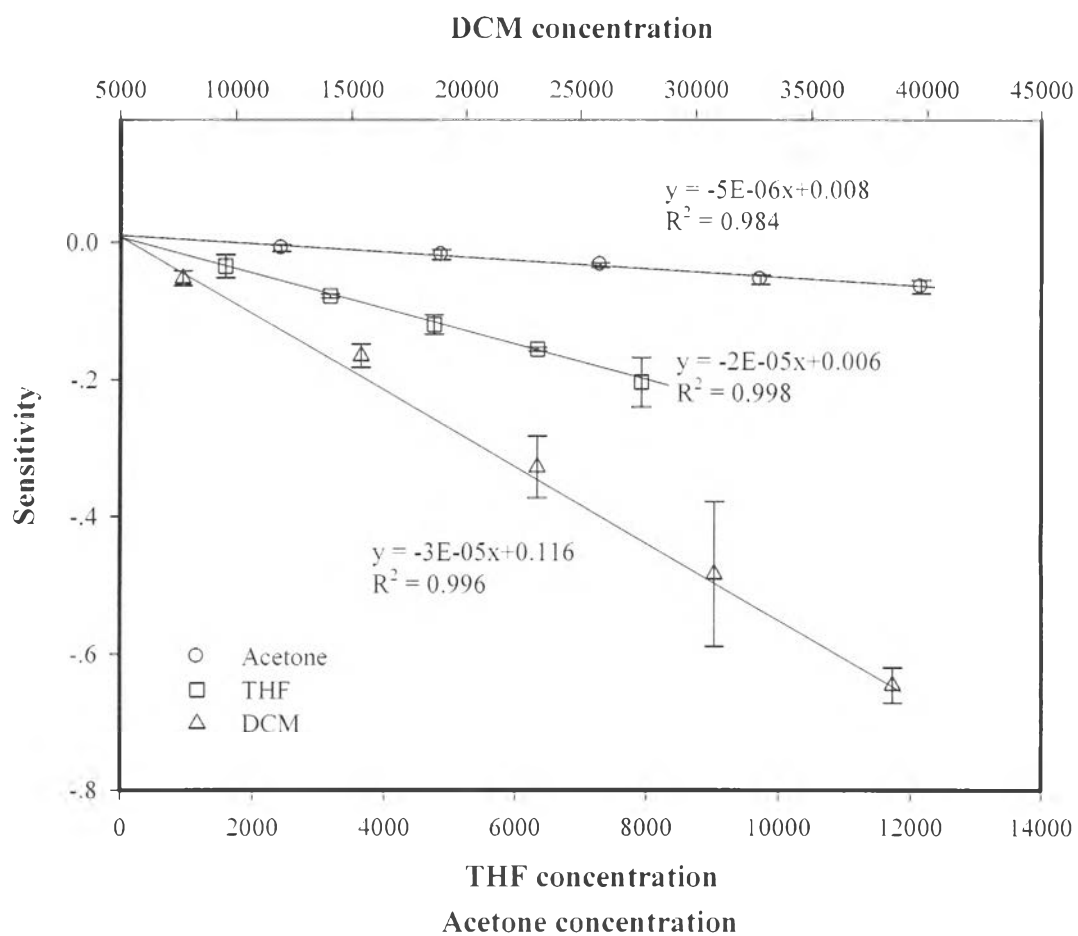
Figure 6.5 Sensitivity of nPDPA-SDS_1-0.5/15%DYH[80] composite toward DCM. THF. and acetone vapors at different concentrations at 27±1 °C and 1 atm.
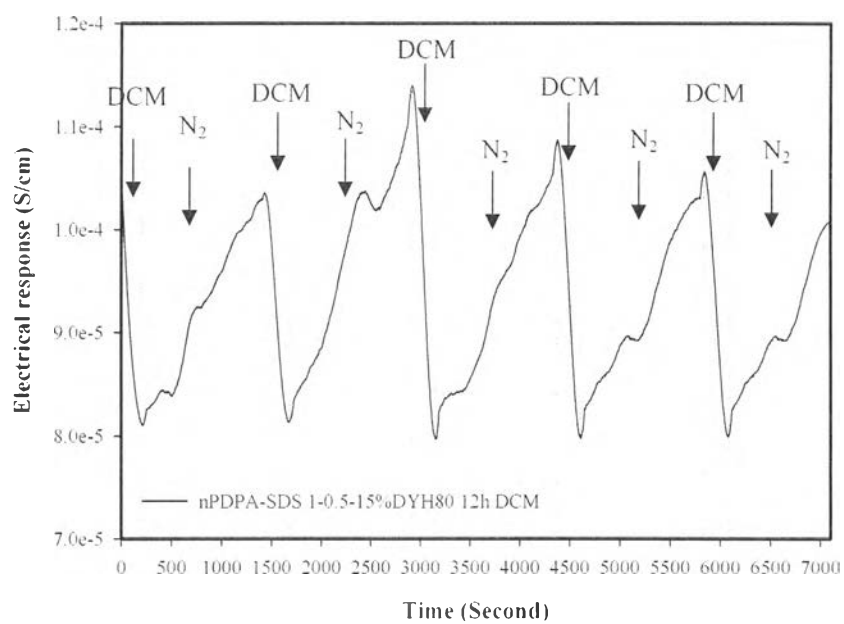
Figure 6.6 Negatively cyclic responses of nPDPA-SDS_1-0.5/15%DYH[80] composite exposed to 50 %v/v DCM vapor at 27 °C. 70 %RH.
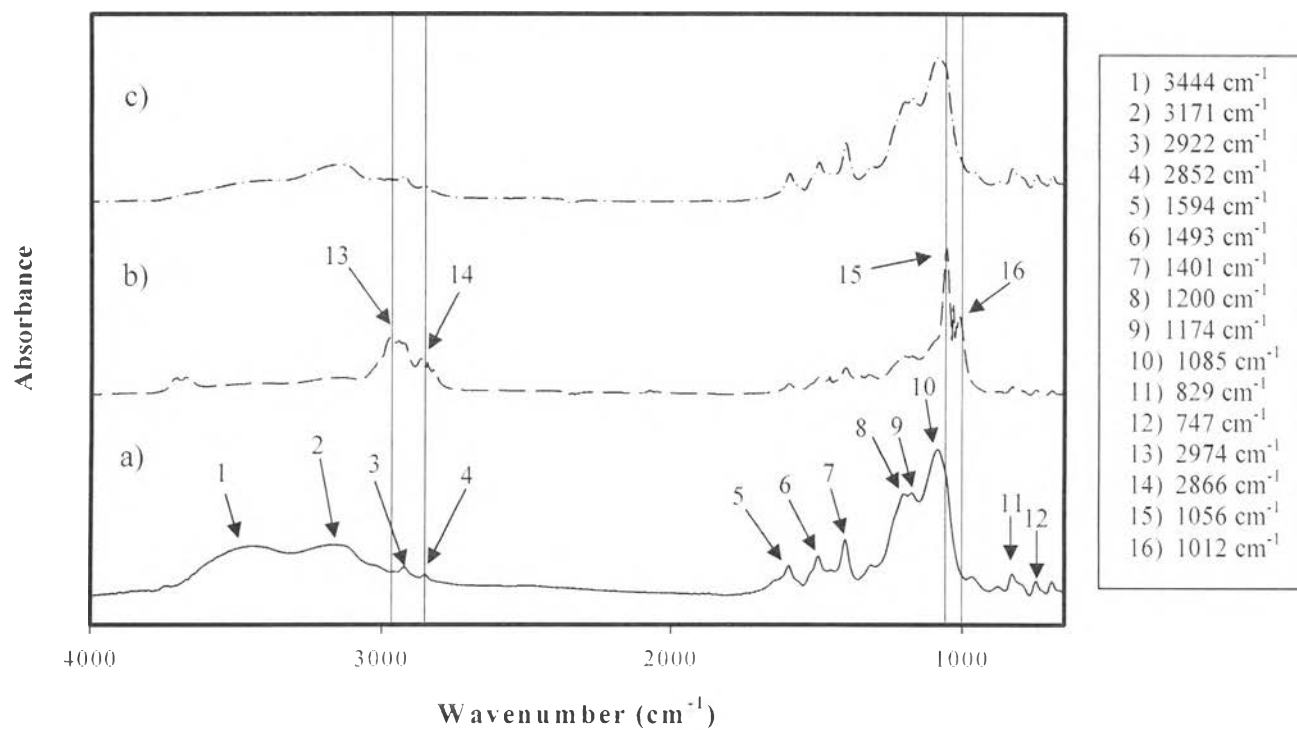
Figure 6.7 FT-IR spectra of nPDPA-SDS_1-0.5/15%DYH[80] composite: a) before;
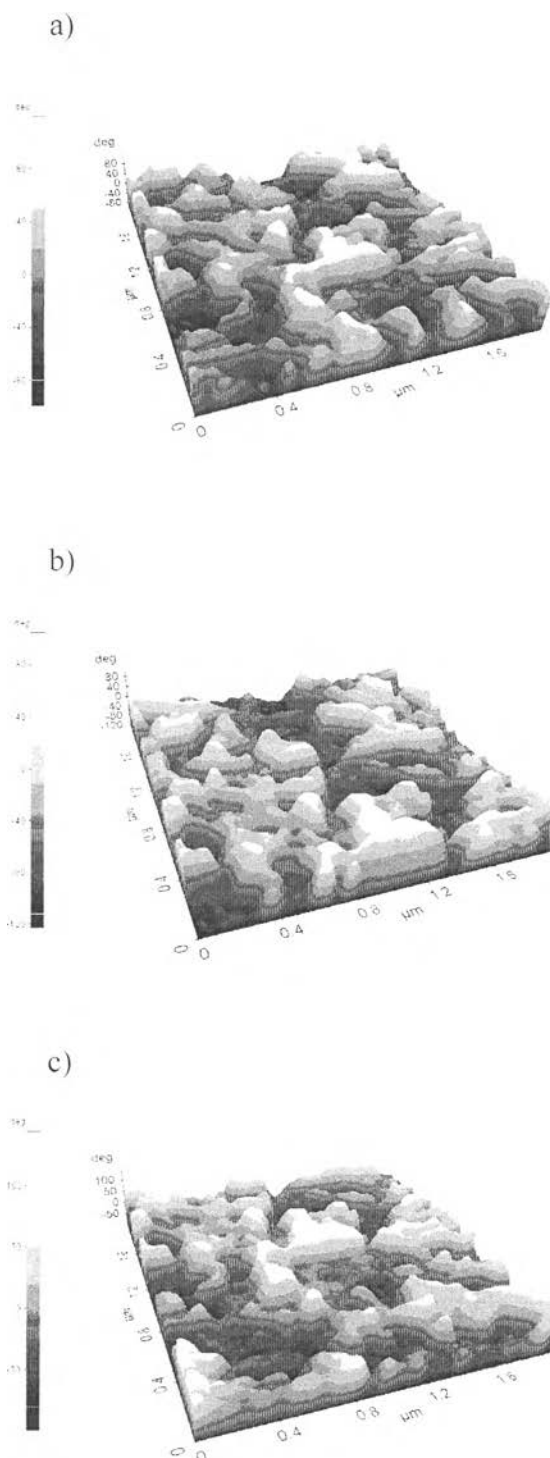b) during; and c) after exposed to DCM at 27 °C, 70 %RH.

a)

b)

c)

Figure 6.8 EFM images of nPDPA-SDS_1-0.5/15%DYH[80] composite: a) before; b) during; and c) after exposed to DCM vapor.
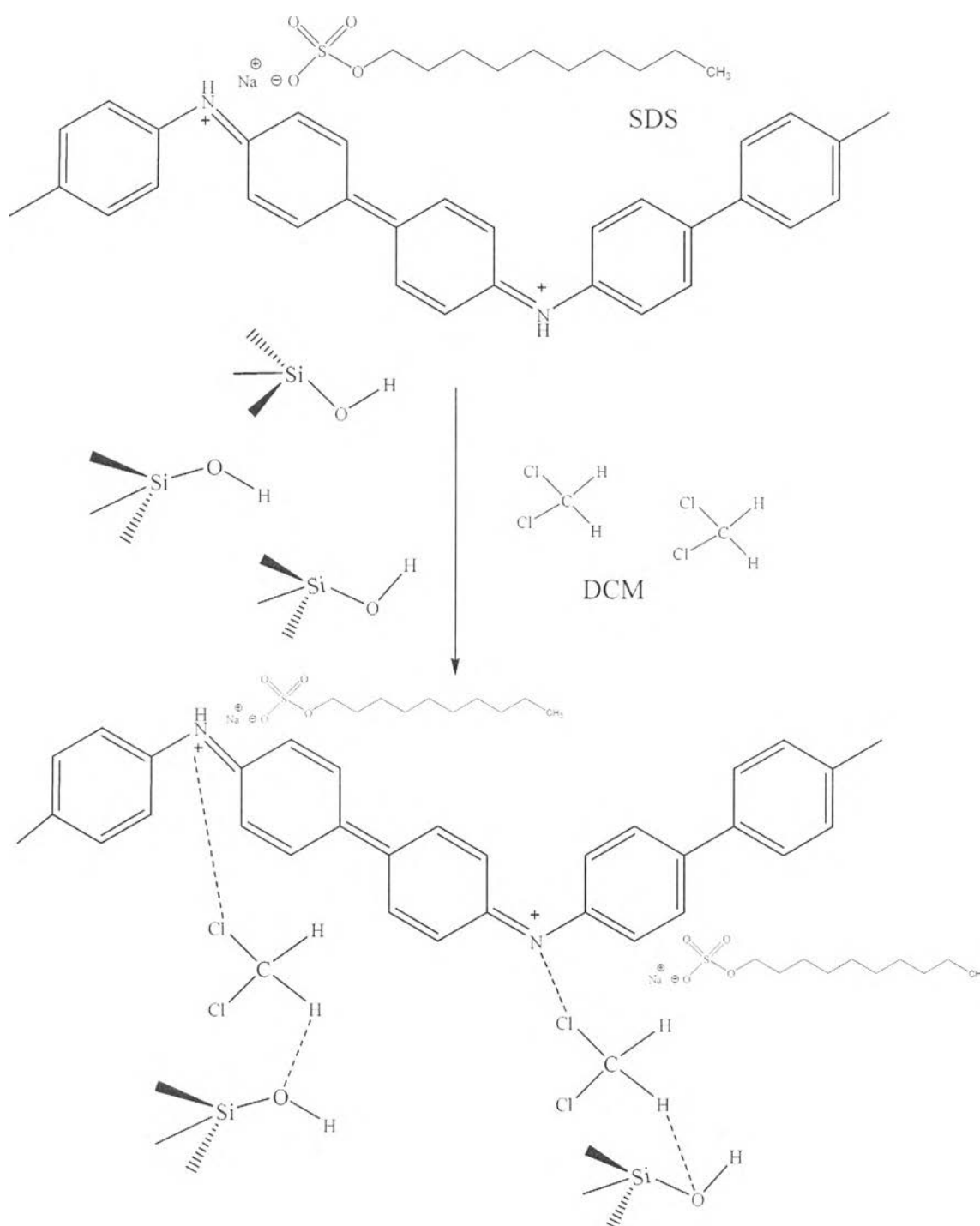
Figure 6.9 Proposed mechanism for the interactions of nPDPA-SDS_1 0.5/15% DYH[80] composite and DCM vapor.

Table 6.1 Sensitivity, induction time (t_i), and recovery time (t_r) of nPDPA-SDS_1-0.5/15%DYH[80] composite when exposed to different solvent vapors

Vapors	Sensitivity (S/cm)	t_i (min)	t_r (min)
Hexane	$(-1.79 \pm 2.39) \times 10^{-2}$	12.94 ± 0.72	12.23 ± 0.31
Toluene	$(-1.54 \pm 2.22) \times 10^{-1}$	7.79 ± 0.32	8.79 ± 0.63
Chloroform	$(-1.55 \pm 2.10) \cdot 10^{-1}$	7.54 ± 0.16	8.23 ± 0.16
DCM	$(-9.76 \pm 0.32) \times 10^{-1}$	5.31 ± 0.07	6.35 ± 0.17
THF	$(-4.76 \pm 0.94) \cdot 10^{-1}$	6.78 ± 0.48	7.44 ± 0.17
Acetone	$(-4.29 \pm 2.39) \cdot 10^{-1}$	7.88 ± 0.49	8.39 ± 0.10
DMF	$(-1.18 \pm 1.51) \cdot 10^{-1}$	6.95 ± 0.57	7.18 ± 0.71
Methanol	$(-2.63 \pm 2.33) \cdot 10^{-2}$	10.84 ± 0.55	10.15 ± 0.71
Ethanol	$(-2.10 \pm 2.56) \cdot 10^{-2}$	10.94 ± 0.69	11.63 ± 0.56
Propanol	$(-1.76 \pm 0.89) \cdot 10^{-2}$	11.34 ± 0.86	11.45 ± 0.16

Table 6.2 Physical properties of the solvents tested

Solvent	Polarity	Dielectric constant	Dipole moment	Solubility parameter $(MPa^{1/2})$
Hexane	0.10	1.88	0.00	14.9
Toluene	2.40	2.38	0.36	18.2
Chloroform	4.10	4.81	1.04	18.7
DCM	3.10	9.10	1.60	20.2
THF	4.00	7.50	1.75	19.4
Acetone	5.10	21.00	2.88	19.7
DMF	7.20	38.00	3.82	24.9
Methanol	5.10	33.00	1.70	29.6
Ethanol	5.20	24.55	1.69	26.5
Propanol	4.00	20.00	1.68	24.6

*solubility parameter of nPDPA is 20.8 $MPa^{1/2}$ (Permpool *et al.*, 2013)